Numerical simulation of turbulent flow in a cyclonic separator

Dmitry Bogdanov and Sergey Poniaev

Division of Plasma Physics, Atomic Physics and Astrophysics, Ioffe Physical Technical Institute, 26 Polytekhnicheskaya, St Petersburg 194021, Russian Federation

E-mail: dimyriy.bogdanov@gmail.com

Abstract. Abstract. Numerical simulation of a turbulent flow of air with dispersed particles through a cyclonic separator is presented. Because of a high streamline curvature in the separator it is difficult to simulate the flow by using the conventional turbulent models. In this work the curvature correction term was included into the $k-\omega-SST$ turbulence model implemented in the OpenFOAM® software. Experimental data and results of numerical simulation by the commercial ANSYS Fluent® solver for a turbulent flow in a U-duct were used to validate the model. The numerical simulation of the flow in the cyclonic separator demonstrates that the implemented turbulence model successfully predicts the cyclonic separator efficiency.

1. Introduction

Cyclonic separators are widely used for dispersed phase separation from the gas [1] . One of their important parameters is the efficiency which is the ratio between the number of filtered particles and the total number of particles injected into a cyclonic separator. However, it is extremely difficult to predict the separator efficiency by using numerical simulation of the turbulent flow because conventional eddy-viscosity models cannot adequately describe the flow [2] because of a high streamline curvature and, more specifically, inadequate calculation of the turbulence kinetic energy production. The kinetic energy production can be corrected by using the Shur-Spalart curvature correction function for the Spalart-Allmaras turbulence model reformulated in [3] in terms of the $k-\omega-SST$ turbulence model.

2. Cyclonic separator model

The typical scheme of the air flow in cyclonic separator is presented on Figure 1 [1]. The air with dispersed particles enters the cyclone through air inlet. Under the centrifugal forces the heavy particles pass near to the boundary layer on a sidewall. It that region the influence of the air flow on particles movement is relatively small in compare with influence of the gravity forces and particles falling down to the dust. Cleaner air goes out from cyclone through air outlet.

3. SST with curvature correction model formulation

The correction function (1) suggested in [2] used as a multiplier of the production term in the Spalart-Allmaras eddy viscosity transport equation.

$$f_{rotation} = (1 + c_{r_1})\frac{2r^*}{1 + r^*}[1 - c_{r_3}\tan^{-1}(c_{r_2}\tilde{r})] - c_{r_1} \tag{1}$$

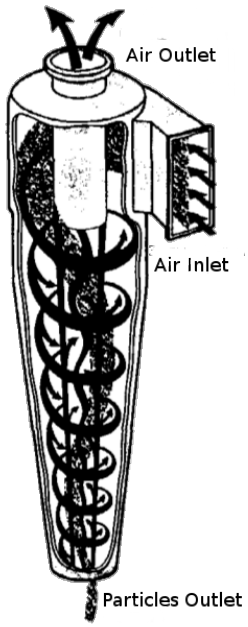

Figure 1: Scheme of the air flow inside cyclonic separator.

Article [3] suggests to use this function as follows in respect to the SST model.

$$\frac{\partial(\rho k)}{\partial t} + \frac{\partial(\rho u_j k)}{\partial x_j} = P_k f_{r_1} - \beta^* \rho k\omega + \frac{\partial}{\partial x_j}\left[\mu_{eff}\frac{\partial k}{\partial x_j}\right] \tag{2}$$

$$\frac{\partial(\rho \omega)}{\partial t} + \frac{\partial(\rho u_j \omega)}{\partial x_j} = \alpha\frac{\rho P_k}{\mu_t} f_{r_1} - D_\omega + Cd_\omega + \frac{\partial}{\partial x_j}\left[\mu_{eff}\frac{\partial \omega}{\partial x_j}\right] \tag{3}$$

$$f_{r_1} = \max\left[\min(f_{rotation}, 1.25), 0\right] \tag{4}$$

$$r^* = \frac{S}{\Omega} \tag{5}$$

$$\tilde{r} = 2\Omega_{ik}S_{jk}\left[\frac{DS_{ij}}{Dt} + (\varepsilon_{imn}S_{jn} + \varepsilon_{jmn}S_{in})\,\Omega_m^{rot}\right]\frac{1}{\Omega D^3} \tag{6}$$

$$S_{ij} = \frac{1}{2}\left(\frac{\partial u_i}{\partial x_j} + \frac{\partial u_j}{\partial x_i}\right) \tag{7}$$

$$\Omega_{ij} = \frac{1}{2}\left(\left(\frac{\partial u_i}{\partial x_j} - \frac{\partial u_j}{\partial x_i}\right) + 2\varepsilon_{mji}\Omega_m^{rot}\right) \tag{8}$$

$$S^2 = 2S_{ij}S_{ij}, \quad \Omega^2 = 2\Omega_{ij}\Omega_{ij} \tag{9}$$

$$D^2 = \max(S^2, 0.09\omega^2) \tag{10}$$

DS_{ij}/Dt - components of the Lagrangian strain tensor derivative.

$$c_{r_1} = 1.0, \quad c_{r_2} = 2.0, \quad c_{r_3} = 1.0$$

4. Model validation

Turbulence model described in Section 3 has been implemented using OpenFOAM® mathematical library. Numerical simulation results comparison with Monson [4] experimental data for turbulent flow in U-duct and numerical simulation in ANSYS Fluent® for the velocity projections U_x and U_y shown in Figures 3 to 6. U-duct geometric and flow parameters shown in Table 1. Flow scheme presented in Figure 2. At the inlet section in accordance with the experiment the flow was assumed fully developed. So inlet profiles used as inlet boundary condition were obtained from preliminary computations of the turbulent flow in a plane channel.

It can be seen that the results of numerical simulation obtained using both implemented model and ANSYS Fluent® solver are in good agreement with the Monson experimental data. SST model with curvature correction shows significant improvement of simulated velocity profile compared to the non-modified SST model.

Table 1: Geometric and flow parameters for air flow in U-duct.

Channel height, H	$3.81cm$
Channel length, L	$10H$
Inner radius, R_i	$1.91cm$
Outer radius, R_o	$5.72cm$
Average velocity at inlet U_{in}	$30.1m/s$
Average temperature at inlet, T_{in}	$264K$
Pressure at outlet, p_{out}	$1.15atm$
Reynolds number, Re	10^5

Figure 2: Scheme of air flow in U-duct

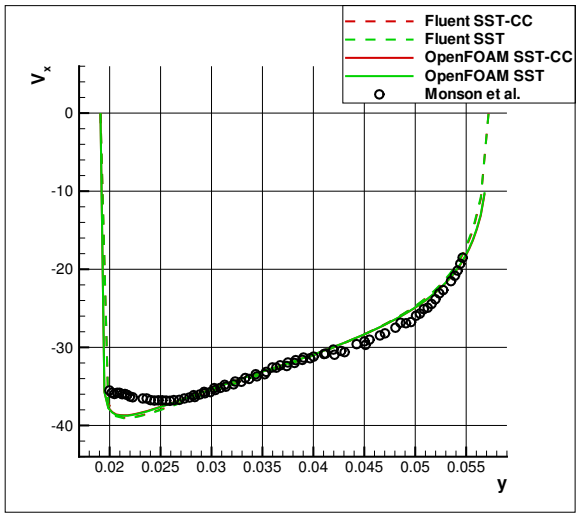

Figure 3: U_x, $x/H = 0$ (lower channel)

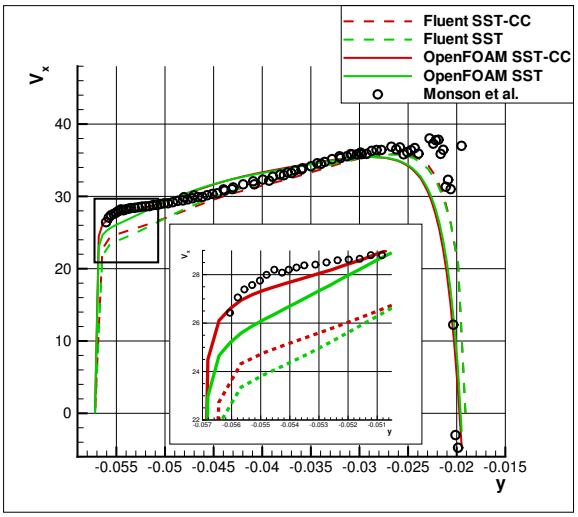

Figure 4: U_x, $x/H = 0$ (top channel)

5. Results

In this section we consider the flow in cyclonic separator shown in Figure 7. Geometric parameters and boundary conditions presented in Table 2 and Table 3 respectively. Inlet velocity profile obtained from computation of fully developed turbulent flow in square-section channel.

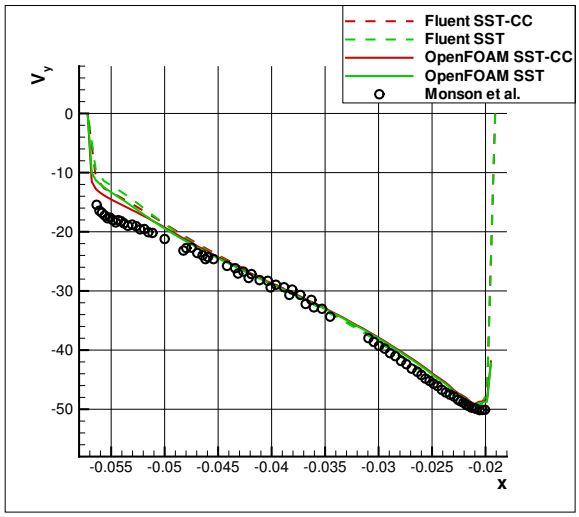

Figure 5: U_y, $y/H = 0$

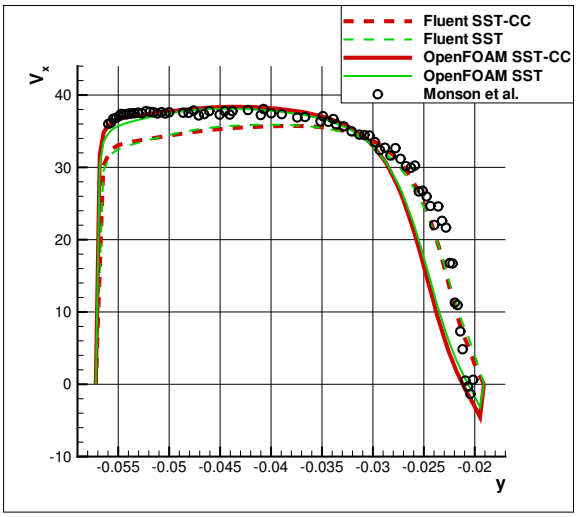

Figure 6: U_x, $x/H = 1$

Solution has been obtained for three different velocities and three different particle diameters. Results of the numerical simulation, compared with the Dirgo and Leith[5] experimental data presented in Table 4. As can be seen from the table, results of the numerical simulation are in good agreement with the experimental data. As might be expected, cyclone efficiency degrades in direct ratio with particles diameter. For diameter $\leq 10^{-7}m$ cyclone is not applicable at all, but for diameter $\geq 10^{-5}m$ it shows almost 100% efficiency. With the decrease of the inlet velocity, cyclone efficiency also degrades due to decreasing influence of a centrifugal force.

Results of particle distribution presented in Figures 8 and 9. Particles with diameter $\leq 10^{-7}$ almost uniformly distributed inside filter which apparently means that influence of centrifugal forces is not large enough to filter out significant part of particles. In opposite, particles with diameters $\geq 10^{-5}$ distributed mostly inside boundary layer on filter sidewall and can be filtered out.

According to the calculation results we can make a conclusion that curvature correction function, suggested in [2], reformulated in [3] and implemented using OpenFOAM in current paper, can be successfully used for simulation of turbulent flows with high streamlines curvature.

Table 2: Cyclone geometric parameters

Cylinder diameter,	$D = 0.205m$
Outlet diameter,	$D_e = 0.5D$
Inlet channel height,	$a = 0.5D$
Inlet channel width,	$b = 0.2D$
Inlet channel length,	$h_e = 0.75D$
Total filter height,	$H = 4.0D$
Cylinder height,	$h = 1.5D$
Lower section diameter,	$B = 0.36D$
Dust height,	$h_d = 0.25D$
Dust diameter,	$D_d = 0.75D$

Table 3: Cyclone Flow parameters

Inlet velocity,	$U_{in} = 5, 10, 15, 20m/s$
Inlet temperature,	$T_{in} = 300K$
Particles temperature,	$T_{p_{in}} = T_{in}$
Particles inlet velocity,	$U_{p_{in}} = U_{in}$
Outlet pressure,	$P_{out} = 1atm$
Wall heat transfer,	$q_w = 0$
Particles diameters,	$d_p \sim 10^{-5}m, 10^{-6}m, 10^{-7}m$

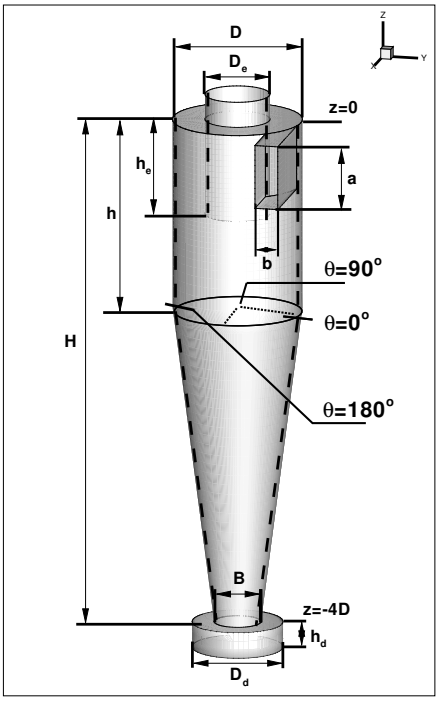

Figure 7: Cyclone scheme

Table 4: Cyclonic separator efficiency η comparison

Flow parameters	η, Numerical simulation	η, Experiment
$U_{in} = 20m/s, d = 5 \cdot 10^{-5}m$	100%	100%
$U_{in} = 20m/s, d = 5 \cdot 10^{-6}m$	93%	90%
$U_{in} = 20m/s, d = 5 \cdot 10^{-7}m$	27%	10%
$U_{in} = 15m/s, d = 10^{-5}m$	80%	90%
$U_{in} = 10m/s, d = 10^{-5}m$	72%	85%
$U_{in} = 5m/s, d = 10^{-5}m$	75%	80%

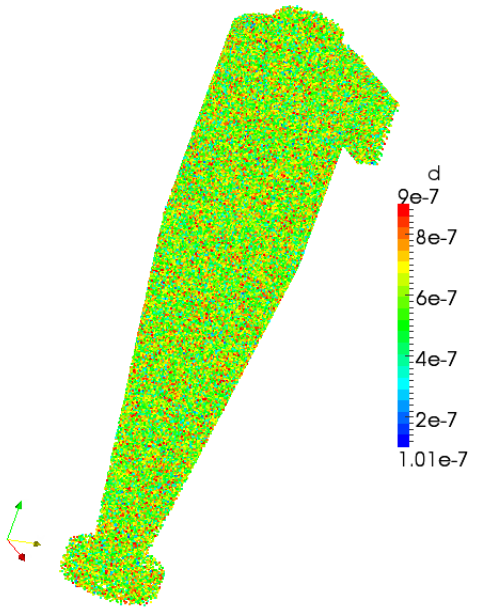

Figure 8: Particles distribution for $d \sim 10^{-7}$ $U_{in} = 20m/s$

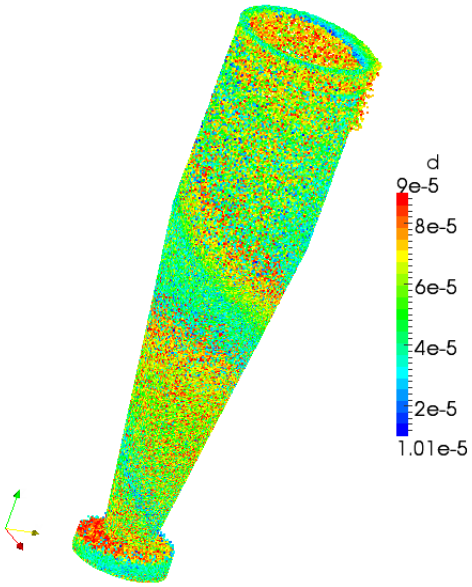

Figure 9: Particles distribution for $d \sim 10^{-5}$ $U_{in} = 20m/s$

References

[1] Uzhov V 1970 *Yaroslavl*
[2] Spalart P and Shur M 1997 *Aerospace Science Technology* **15**
[3] Smirnov P and Menter F 2009 *Journal of Turbomachinery* **131**
[4] Monson D, Seegmiller H, McConnaughet P and Chen Y 1990 *AIAA Paper* **21**
[5] Dirgo J and Leith D 1985 *Aerosol Sci. Tech.* **4** 410415